Investigation of potential polyatomic interferences on uranium isotope ratio measurements for the LS-APGD-Orbitrap MS system

Joseph V. Goodwin[1], Benjamin T. Manard[2*], Brian W. Ticknor[2], Paula Cable-Dunlap[3], and R. Kenneth Marcus[1*]

1. Department of Chemistry, Clemson University, Clemson SC 29634
2. Chemical Sciences Division, Oak Ridge National Laboratory, Oak Ridge, Tennessee 37830
3. Nuclear Nonproliferation Division, Oak Ridge National Laboratory, Oak Ridge, Tennessee 37830

[*]Corresponding Authors: B.T. Manard, manardbt@ornl.gov; R. Kenneth Marcus, marcusr@clemson.edu

Manuscript to be submitted to Microchemical Journal

Keywords: uranium, LS-APGD, Orbitrap, mass spectrometry, nuclear, safeguards

Abstract

The determination of actinide (e.g., U and Pu) content and isotopics is of importance to the nuclear forensics and safeguards communities. However, in the analysis of environmental samples, such as those collected by the International Atomic Energy Agency, uranium measurements can be complicated by isobaric interferences from polyatomic variants of heavy elements (e.g., Pb). This leads to complex, time-consuming sample manipulations (i.e., separations) before determining isotope ratios. An alternative strategy to sample pretreatment is to use high-resolution mass spectrometric platforms during the analysis to fully resolve the uranium isotopes from potential polyatomic interferences, negating the need for prior chemical separation. The liquid sampling - atmospheric pressure glow discharge (LS-APGD) coupled with an Orbitrap mass spectrometer provides a high-resolution (> 70,000 m / Δm at m/z 200) inorganic mass spectrometry platform. As a demonstration of the power of this instrumental platform, and indeed, the high-resolution approach in general, uranium isotope ratios were determined in the presence of elemental impurities (e.g., Pb, Pt, Ta, W) commonly encountered with environmental sample swipe analysis, without any prior treatment. Even at elemental impurity concentrations of 1000-5000× relative to uranium, no interference was observed with the ^{235}U or ^{238}U signal. In addition, the $^{235}U/^{238}U$ isotope ratio for the samples with the concomitants present are within 2 standard deviations of the values obtained without their addition, indicating that these impurities do not impact the determined uranium isotope ratio. These findings represent a significant first step in leveraging the high resolution of the LS-APGD-Orbitrap-MS to overcome isobaric and molecular interferences instead of relying on chemical separations.

1. Introduction

Accurate and precise isotopic determination of actinides (e.g., uranium and plutonium) from environmental sampling (ES) substrates, including cotton swipes, vegetation, soils, biota, etc., is routinely employed as part of the international nuclear safeguards regime [1,2]. ES cotton swipes are a common sampling methodology for safeguards that can be used to collect traces of nuclear material present in facilities under safeguards and are a powerful method for detecting the presence of undeclared material and/or activities. Typically, these samples are analyzed in two categories: bulk or particle-workflows [3]. For the ES bulk measurements, the sample is processed in its entirety (as opposed to analyzing individual particles) and measured for U and Pu concentration and isotopic content. This analysis protocol is laborious and generally consists of sample/substrate ashing, digestion, separations via column chromatography, matrix conversion, and subsequent analysis by high-resolution ($m/\Delta m \sim 10{,}000$) multi-collector inductively coupled plasma (MC-ICP) or thermal ionization mass spectrometry (TIMS).

Due to its sensitivity and throughput, MC-ICP-MS is often preferred for this routine measurement; however, it does have some limitations. Commonly, in ICP-MS measurements, isobaric and molecular inferences are notorious for hindering the analysis of low-mass elements, for example, $^{12}C^{12}C$ and ^{24}Mg; ^{40}Ar and ^{40}Ca; and $^{40}Ar^{16}O$ and ^{56}Fe, to name a few. The analysis of high-mass elements, including U, can also be hindered by polyatomic interferences, particularly when heavy elements (e.g., Pb, Hg, W, Pt) are present. These species of concern are typically in the form of MH^+, MO^+, and MOH^+. Pointurier et al. [4] and Pollington et al. [5], have outlined these interferences in great detail. The presence of such heavy elements, as well as co-actinide molecular interferences (e.g., ^{238}UH and ^{239}Pu), necessitate these chemical separation(s) steps.

One approach, a combination of TEtra VAlent (TEVA) and uranium TEtra VAlent (UTEVA), has proven effective for this separation [6]. While some work has been dedicated to automating this process [7], a typical separation procedure will take ~1 week.

Recent research efforts in nuclear analytical chemistry have explored the utilization of triple quadrupole (TQ) – ICP-MS to alleviate the hindrances of molecular and polyatomic interferences when targeting trace elements [8], anions [9,10], and actinide measurements [11-14]. In general, this approach has proven to be successful in the determination of trace elements, and it is routinely employed [15]. For actinide determinations, a separation is still typically employed prior to the TQ-ICP-MS analysis. It has been documented that, while gasses such as CO_2 are very efficient at mass-shifting U ions, they will typically react with Pu at a rate of ~50% [16,17], ultimately hindering high sensitivity measurements. Another approach to addressing isobaric and molecular interference is using high-resolution mass analyzers. In traditional inorganic mass spectrometry (e.g., ICP-MS), a magnetic sector–based mass analyzer is utilized, typically achieving a mass resolution of up to $R = m / \Delta m \sim 10{,}000$ [18]. This can be a powerful approach when measuring trace elements in nuclear materials [8,19], but the reduction of sensitivity by ~50× (when employing high-resolution mode) limits its application in the determination of trace actinides; ultimately, higher resolution without a corresponding drop in sensitivity would be warranted for these actinide-based isobaric interferences. Currently, chemical separations remain a pre-requisite in most actinide element determinations.

In an effort to alleviate isobaric and molecular interferences in isotope ratio analysis, ultrahigh-resolution ($m / \Delta m$ ~70,000) Orbitrap mass analyzers have been

implemented in the field of inorganic mass spectrometry in conjunction with a microplasma ionization source, the liquid sampling – atmospheric pressure glow discharge (LS-APGD) [20,21]. This novel platform has demonstrated its analytical usefulness in the fields of nuclear [22-24] and geochemistry [25],. Indeed, the advantages of high-resolution determinations with the LS-APGD / Orbitrap coupling were clearly demonstrated by resolving ^{87}Sr from ^{87}Rb using a high-field Orbitrap having an operating resolution of >1,000,000 [25]. The LS-APGD is not restricted to the analysis of infused solutions; in fact, the source has a rich history of surface analysis techniques, including the analysis of laser ablation particles [26,27] and direct surface desorption [28,29]. In addition, the LS-APGD has been used for the isotopic measurements of uranium directly from environmental swipe surfaces by using a novel surface sampling microextraction probe [30] developed initially for mass spectrometric analysis from thin-layer chromatography plates. The microextraction technique has been successfully applied to isotopic measurements of uranium and plutonium directly from environmental swipes using quadrupole and sector field ICP-MS platforms [31-34]. The results were extremely promising; however, all measurements were made without interfering elements, only uranium or plutonium-containing material was present. Since traditional methods of sample pretreatment to remove isobaric interferences were not practical when directly sampling a material on a surface, a correction factor for $^{238}U^{1}H$ was applied to the measurement of ^{239}Pu from mixed U/Pu samples, which hindered the performance of the Pu measurement compared to unmixed case [34]. With the LS-APGD Orbitrap platform, high-resolution mass spectrometry, instead of sample pretreatment, can be used to differentiate between isobaric species.

The LS-APGD/Orbitrap coupling may be able to alleviate the need for extensive separation chemistries prior to actinide analysis. This would be an important advance in terms of sample throughput in the analyses of solutions and direct sampling of ES swipes. Here we evaluate the LS-APGD-Orbitrap MS platform with regard to mass-resolving interferences associated with problematic elements commonly found in ES swipes [4,5]. A uranium isotopic standard was mixed with excess amounts (1000-5000×) of high-mass trace elements (e.g., Pb, Pt, Ta, and W) and was analyzed via the LS-APGD-Orbitrap MS platform, *without any prior sample pretreatment*. This evaluation involves two considerations; identification of the various ionic species generated from each element by the LS-APGD source and then verification that such species are not impactful in the uranium determinations. As documented in previous efforts, the product molecular ions produced in the microplasma are very different from those derived from an ICP source [20,35]. These results ultimately illustrate the power of using the LS-APGD microplasma with extremely high-resolution inorganic mass spectrometer platforms to overcome isobaric interferences instead of relying on complex sample manipulations before measurement. This work marks a significant step towards determining uranium isotope ratios directly from environmental swipes possibly in an in-field setting, as sample pretreatment is not required to overcome isobaric interferences from commonly encountered elemental impurities.

2. Material and Methods

2.1 Solution Preparation

A dilute (2%) nitric acid solution was used as a diluent and a blank for all studies. The 2% nitric acid solution was prepared by diluting 70% Airstar ultra-trace nitric acid

(BDH/VWR, Radnor, PA) with ultra-trace water (BDH/VWR, Radnor, PA). Pt, Ta, and W solutions were diluted from stocks obtained from High Purity Standards (Charleston, SC), while a Pb stock was obtained from CPI International (Santa Rosa, California). Stock solutions of Pb, Pt, Ta, and W were prepared at 10 μg mL^{-1} for collisional dissociation studies. Two low-enriched certified uranium solutions (IRMM-202X series) were obtained from JRC (Geel, Belgium, formally the Institute for Reference Materials and Measurements) [36]. IRMM-2028 ($^{235}U/^{238}U$ of 0.037576) was used for spiking studies, while IRMM-2027 ($^{235}U/^{238}U$ of 0.041717) was used for mass bias corrections. For isotope ratio measurements, solutions containing IRMM-2028 and IRMM-2027 (mass bias solution) were prepared at an elemental concentration of 10 ng mL^{-1}; these solutions were analyzed free from any added elemental impurities to establish an IRMS baseline. Mass bias corrections were made utilizing a direct mass bias correction method, similar to Mathew et al. [37]. For spiking studies, solutions were prepared which consisted of 10 ng mL^{-1} of IRMM-2028 and 10 ug mL^{-1} of each elemental impurity (one elemental impurity per solution), representing a 1000× excess in the potential elemental interferents with respect to uranium. In addition, spiking studies were conducted with 10 ng mL^{-1} of IRMM-2028 and 50 ug mL^{-1} of Ta and W, which represent a 5000× excess in these concomitants with respect to uranium.

2.2 Liquid Sampling-Atmospheric Pressure Glow Discharge (LS-APGD)

A dual-electrode liquid sampling-atmospheric pressure glow discharge (LS-APGD), as previously described [38] and presented in Fig. 1, was used during the course of this study. The LS-APGD is positioned in front of the Orbitrap mass spectrometer's ion transfer capillary (ITC). The LS-APGD's solution cathode consists of an outer stainless-

steel tube (0.4 mm ID, 1.6 mm OD, McMaster Carr, Elmhurst, IL) and an inner fused silica capillary (250 µm ID, 360 µm OD, Molex, Lisle, IL). The outer capillary delivers the helium (Ultra High Purity, Airgas, Radnor, PA) sheath gas to the plasma, while the inner capillary delivers the electrolyte solution. The two positively-powered electrodes (anodes) are stainless steel weldable feedthroughs (MDC Vacuum Products, LLS, Haywood, California). The plasma is struck between the grounded solution (cathode) and the two powered anodes. A custom control box developed by GAA Custom Electronics, LLC (Kennewick, WA) controls the solution flow rate, sheath gas flow rate, and provides constant current to the powered anodes. For all studies, a helium sheath gas flow rate of 500 mL min^{-1}, a solution flow rate of 30 µL min^{-1}, and a current of 30 mA was employed.

2.3 Orbitrap Mass Spectrometer

A Thermo Scientific Q Exactive Focus Orbitrap was used during this study. No modifications were made to the instrument other than the removal of the manufacturer's electrospray ionization source, allowing direct coupling of the LS-APGD ionization source. Prior to all measurements, the instrument was allowed to "warm up" for approximately 30 minutes while the plasma was operated on a direct infusion of electrolyte (2% HNO_3) solution. Typical for uranium isotope ratio determinations with the LS-APGD, 90 eV of in-source collisional dissociation (CID) energy and 120 eV of higher-energy collisional dissociation energy (HCD) was applied for isotope ratio determinations and, when applicable, during the collisional dissociation studies [23] . The ion transfer capillary temperature was set to 250°C. The resolution of the mass spectrometer was set to $m/\Delta m$ = 70,000 (at m/z of 200), the maximum injection time was set to 100 ms, and the automatic gain control (AGC) target was set to 1 million charges. 10 microscans were collected per

scan, wherein each microscan represents a single ion packet injection into the Orbitrap mass analyzer. Two sets of conditions were used, one for collisional dissociation studies and one for isotope ratio measurements. For collisional dissociation studies, the scan range was set to 150-400 m/z, and 4-minute direct infusions were used. When HCD was used during the collisional dissociation studies, a quadrupole range of 150-400 m/z was employed. Uranium isotope ratio determinations were performed using the uranium dioxide cation ($UO_2^{+)}$ as the target species, typical for uranium isotope ratio measurements with the LS-APGD / Orbitrap. For uranium isotope ratio determination, the standard conditions were used; specifically, 900 scans (approximately 45 minutes) direct infusions were employed with a quadrupole range of 268.5 ± 25.0 Da and a digitization range of 268.5 ± 5.0 Da [23,39]. A 600-point moving average was applied to the 900 scans from the transient signal collected during each analysis. The moving average process is described in detail elsewhere [23].

3. Results and Discussion:

3.1 Characterization of Potential Interferences and Effects of Collisional Dissociation

Different from mass spectrometer platforms common to ICP-MS, where multi-quadrupole/reaction cells are employed to effect chemical reactions or kinetic energy discrimination of isobars [40-42], the Orbitrap mass spectrometer is equipped with two modes of collisional dissociation to affect their removal. In-source collisional dissociation (CID) occurs when ions are accelerated in a nitrogen-filled region between the exit lens of the S-lens and the injection flatapole. Higher-Energy collisional dissociation (HCD) occurs when the C-trap-collected ions are accelerated into a nitrogen-filled collision cell.

Product ions are then returned to the C-trap for injection into the Orbitrap mass analyzer. Previous studies investigating the use of CID and HCD with the LS-APGD showed that CID was effective at removing waters of hydration from the metallic analyte, while HCD is capable of dissociating molecular species [43]. As shown in Fig. 1, one of the key differences between these collisional modalities is their placement in the ion beam path, with CID occurring before the quadrupole mass filter. Since the HCD cell is after the quadrupole mass filter, HCD dissociation is only applied to ions permitted to pass through the quadrupole mass filter; all other ions are rejected by the quadrupole. Since this study is primarily focused on uranium isotope ratio measurements, no optimization of the primary collisional dissociation parameters is needed; the typical conditions of CID energy (90 eV), quadrupole range (268.5 ± 25.0 Da), and HCD energy (120 eV) used for routine uranium isotope ratio analysis [43,22].

Four commonly encountered elemental impurities when performing uranium isotope ratio determinations from environmental swipes, Pb, Pt Ta, and W, were used to evaluate the LS-APGD / Orbitraps' ability to use high mass resolution to overcome potential impurities. The natural first step to understanding what impact these elemental impurities might have with uranium isotope ratio measurements is to understand their native mass spectra and how those native species dissociate using the typical settings for CID, HCD, and quadrupole mass filter bandpass used in U isotope ratio measurements. First, each element was analyzed in its native state without applying any type of collisional dissociation energy. The native spectrum for a 10 μg mL^{-1} solution of Pb is shown in Fig. 2a, for Pt in Fig. 3a, for Ta in Fig 4a, and for W in Fig. 5a. The shaded regions in each spectrum represent the quadrupole range (268.5 ± 25.0 Da) employed

during uranium isotope ratio analysis for each figure. Only species within the quadrupole range would be permitted to pass through to the HCD cell and finally onto the Orbitrap mass analyzer, so only species within the quadrupole range have the potential to cause interferences with uranium isotope ratio measurements. As can be seen, none of the target elements exists predominantly in the M^+ state, but instead are present as oxides or as H_2O/NO_3-related clusters. Pb exists predominantly as $[Pb+NO_3]^+$ in the native spectrum, while Pt exists as PtO_4 with 1 or 2 water clusters. Ta is predominantly TaO_2 as a cluster with two water molecules. W is observed as either $[WO_2+H_2O+OH]^+$ or as $[W+3H_2O+OH+NO_2+N_2]^+$. Each of these species is very accurately assigned based on the mass accuracy and resolution provided by the Orbitrap.

Subsequently, each test element solution was analyzed with 90 eV of CID energy applied without using the quadrupole mass filter or any further HCD dissociation. This set of experiments observed how the native spectra changed after applying CID and whether any clusters remained that would fall within the quadrupole range commonly employed for uranium isotope ratio determinations. The product mass spectra obtained following 90 eV CID are shown in Fig. 2b for Pb, Fig. 3b for Pt, Fig. 4 for Ta, and Fig. 5b for W. The shaded region of each plot again represents the quadrupole range (268.5 ± 25.0 Da) employed during uranium isotope ratio analysis. Only species existing within the quadrupole range could potentially cause interference or issues with uranium isotope ratio measurements; all other species existing outside the quadrupole range will be excluded before ever entering the HCD cell. Based on the responses in Figs. 2-5, there is a general decrease in the complexity of species with the application of CID across the test elements. Indeed, for Pb and Pt, the bare elemental peak is the primary peak

following 90 eV CID. The effects of 90 eV of CID are less clear for Ta; the primary peak remains mainly unaffected; however, there is a reduction in the more complex species $[Ta+3O_2+OH]^+$, increasing the fraction of the lower-mass $[TaO_2+3H_2O]^+$ ionic species. Finally, the primary peak is unchanged for W, the more complex ionic species observed in the native spectrum, $[W+H_2O+OH+NO_2+N_2]^+$, was dissociated to an appreciable extent to lower-mass ions as seen in the 90 eV CID spectrum. As shown, each of the potential elemental concomitants has at least one species that will be transmitted through the uranium quadrupole range, such as $[Pb+NO_3]^+$ and $[PtO_4+H_2O]^+$. In particular, the primary ion of Ta $[TaO_2+2H_2O]^+$ lies within the uranium quadrupole range, as well as a significant portion of the species found for W, including the primary ionic species $[WO_2+H_2O+OH]^+$.

As demonstrated previously [43], further dissociation of molecular ion species is possible when HCD energy is applied, affecting metal-coordinated species such as oxides and nitrates as opposed to the waters of hydration principally affected in CID. This point is illustrated in Fig. 6, wherein it is clear that applying 120 eV HCD energy results in a further reduction of Pb-related molecular species. The same level of spectral simplification is seen for each of the other potentially-interfering elements, with any relevant, potentially-interfering species identified in the following experiments.

3.2 Assessment of Potential Spectral Interferences on Uranium Isotopes

After initial studies directed at understanding the efficacy of collisional dissociation, solutions of low-enriched uranium (IRMM-2028) were spiked with each of the potential elemental concomitants at much higher concentrations (10 μg mL^{-1}) relative to the uranium (10 ng mL^{-1}), representing a 1000-fold excess of the spiked elements. As such,

any potential interferences should be exaggerated and readily identified. The mass spectra acquired for each of the element-spiked solutions are presented. Importantly, these spectra are acquired under the exact conditions employed for uranium isotope ratio analysis regarding collisional dissociation, quadrupole band pass, and spectral digitization range. As shown in Figs. 7 a and b for the Pb- and Pt-spiked solutions, no peaks were detected at abundances of greater than 2% relative to the two U isotopic signals. Again, as a point of reference, uranium ICP-MS analysis in the presence of appreciable amounts of Pb would suffer a common problematic isobar at 238 Da of $^{206}PbO_2$ on the monatomic ^{238}U ion [4]. Seen here is the alleviation of isobars by virtue of the different ionization environments between the LS-APGD and the ICP sources. Beyond that, the interferences seen here differ in mass from the target species by greater than 0.5 Da, well beyond any level of expected interference in the identification or quantification of the uranium species for this instrument.

As might be expected from the spectral features shown for Ta and W in Figs. 4 and 5, there are indeed potential interferents in the case of those elements, shown in the spectra presented in Figs. 7c and d. A particularly prominent interfering species is seen in the scale expansion of Fig. 7c, where a peak representing $[^{181}TaO_2 + 3H_2O]^+$ (m/z = 266.97 Da) is significantly more intense than the $^{235}UO_2^+$ peak at m/z = 267.03 Da. Clearly seen, though, the resolution offered by the Orbitrap mass spectrometer is more than adequate to fully resolve the pair; in fact, a resolution of > 4000 $m/\Delta m$ is needed, thus precluding lower-resolution mass spectrometers if trace analyses were performed. As shown in Fig. 7d, W has two very minor-intensity cluster species that are near in mass to each of the $^{235}UO_2$ and $^{238}UO_2$ peaks; however, these peaks are better resolved than

the Ta-related interference shown in Fig. 7c. These clusters are suggested to be $[^{182}W+O2+2H_2O+OH]^+$ at m/z 266.96 and $[^{184}W+O2+3H_2O]^+$ at m/z 269.97. In all, these four elements, which are problematic in the analysis of uranium from environmental samples via ICP-MS, neither produce appreciable isobaric species nor are the overlaps sufficient.

3.3 Uranium Isotope Ratio Measurement in the Presence of Potential Elemental Interferents

While the previous studies illustrate that there are no spectral interferences from Pb, Pt, Ta, or W with uranium, that does not mean that the presence of these elements does not have an impact on uranium isotope ratio determinations. The Orbitrap is an ion-trapping mass spectrometer, and as such, it is susceptible to ion-ion interactions between trapped ions giving rise to space charge effects [44]. The space charge effect's magnitude depends on the number density for all trapped ionic species, both analyte and unwanted concomitant ions, and their proximity in frequency space [45]. Space charge effects due to unwanted concomitant ions pose a higher potential for deleterious effects with Orbitrap mass analyzers than with the quadrupole and sector field mass analyzers. Previous studies of the LS-APGD/Orbitrap coupling have demonstrated that combinations of quadrupole band pass and orbitrap digitization range are effective tools in minimizing/alleviating space charge effects, but ions existing within those band passes for the analytes could be problematic.

To investigate the impact of the potential elemental interferents on uranium isotope ratio determinations, solutions of the elemental spikes at high concentrations (10 μg mL^{-1}) relative to the uranium (10 ng mL^{-1}) were prepared. To further stress the measurements

for the cases where interfering ions were present in the uranium bandpass, the uranium solutions (10 ng mL^{-1}) were spiked with Ta and W at values of 50 µg mL^{-1}, representing elemental concentrations 5000X greater than uranium. A clean (unadulterated) solution of low-enriched uranium IRMM-2028 was analyzed to mimic a clean uranium fraction had the traditional separation techniques been applied. The $^{235}U/^{238}U$ isotope ratio was determined (n=5) to be $^{235}U/^{238}U = 0.0382$ (12), which has a 1.6% relative difference (RD) from the certified value. This measurement allows for a comparison to the isotope ratios obtained for solutions spiked with elemental impurities. The measurement of the 10 ng mL^{-1} uranium solution via direct infusion represents ~13.5 ng total U used for each measurement.

The results of this study are shown in Fig. 8, where the results of the neat IRMM solution are provided by the solid and dashed blue lines, representing the n=5 average values and ±2s range of precision. The certified value of the CRM is given as the dashed grey line. All of the determined isotope ratios for elemental-spiked samples are also presented in Fig. 8, with their respective measurement uncertainty. It should be noted that measurement uncertainty included components of measurement precision and the mass bias correction factor. These measurements are within two standard deviations of the mean value found for the five determinations performed on the un-spiked solution. Each of the impurity spiked solutions had z-scores <1, except for 5000 × W, which had a Z-score of 0.7, meaning that the determined values for the former are within one standard deviation of the neat solution and ~1.3 standard deviations from the mean for the high-concentration W solution. Overall, this result indicates that the values found for the

uranium determinations in the presence of impurities cannot be considered different from the values found for the un-spiked case at the 95% confidence interval.

Conclusions:

This study demonstrated that the combination of the LS-APGD microplasma ionization source and the Orbitrap mass spectrometer can overcome common interferences encountered with traditional mass spectrometric platforms employed for uranium isotope ratio determinations. The elements Pb, Pt, Ta, and W, which produce problematic molecular isobars in uranium IRMS via ICP-MS, including as employed on "high-resolution" MC-ICP-MS instruments, are not manifest, even at concentrations that are up to 5000× those of the uranium analyte. This freedom from interferences is two-fold in nature. First, the types of ionic species generated in the microplasma are very different in chemical composition than those produced in an inductively coupled plasma. Second, the ultra-high resolution provided by this base-level Orbitrap ($m/\Delta m$ ~70,000) is sufficient to alleviate isobaric interferences from those ionic species that survive collisional dissociation on that platform.

While the list of possible elemental species posing potential interference is not exhaustive, it does represent those most common in uranium IRMS. This work demonstrates that this instrumental platform has great potential to reduce the complexity of sample manipulations typically employed for uranium isotope ratio determinations, whether they be for solution-phase or environmental swipe samples. In addition, the Orbitrap used in this experiment is an entry-level Orbitrap. Further improvements in resolution are possible by using higher field Orbitraps, which are capable of higher resolution than the Orbitrap used in this report. Further improvements in resolution,

sensitivity, and IR precisions are possible, even with an entry-level Orbitrap, by using advanced external data acquisition (DAQ), such as the Spectroswiss (Lausanne, Switzerland) FTMS Booster X2 system [46]. Future efforts will include the use of the advanced DAQ and the microextraction methodology to sample environmental swipes directly [30] without the need for exhaustive sample manipulations. In total, this combination of technologies is expected to have a substantial impact on the nuclear forensics and safeguards communities.

Author Contributions

JVG - Methodology, Data Curation, Visualization, Writing – Original Draft Preparation; **BTM –** Methodology, Supervision, Writing – Original Draft Preparation; **BWT** and **PC-D** - Conceptualization and funding acquisition; **RKM -** Conceptualization, Supervision, Writing – Reviewing and Editing. All authors contributed to and approved the manuscript.

Conflicts of Interest

The authors declare no competing financial interests.

Acknowledgments

This work was supported by the Oak Ridge National Laboratory, managed by UT-Battelle for the Department of Energy under contract DE-AC05-000R22725. This work was funded by the United States National Nuclear Security Administration's Office of Defense Nuclear Nonproliferation Research & Development. The authors would like to acknowledge Jacquelyn DeMink (ORNL) for assistance with graphics.

References:

1. Donohue D (1998) Strengthening IAEA safeguards through environmental sampling and analysis. J Alloys Compd 271:11-18
2. Donohue DL (2002) Strengthened nuclear safeguards. Anal Chem 74:28A-35A
3. Boulyga S, Konegger-Kappel S, Richter S, Sangely L (2015) Mass spectrometric analysis for nuclear safeguards. J Anal At Spectrom 30:1469-1489
4. Pointurier F, Hémet P, Hubert A (2008) Assessment of plutonium measurement in the femtogram range by ICP-MS; correction from interfering polyatomic species. J Anal At Spectrom 23:94-102
5. Pollington AD, Kinman WS, Hanson SK, Steiner RE (2016) Polyatomic interferences on high precision uranium isotope ratio measurements by MC-ICP-MS: applications to environmental sampling for nuclear safeguards. J Radioanal Nucl Chem 307:2109-2115
6. Metzger SC, Rogers KT, Bostick DA, McBay EH, Ticknor BW, Manard BT, Hexel CR (2019) Optimization of uranium and plutonium separations using TEVA and UTEVA cartridges for MC-ICP-MS analysis of environmental swipe samples. Talanta 198:257-262
7. Metzger SC, Ticknor BW, Rogers KT, Bostick DA, McBay EH, Hexel CR (2018) Automated separation of uranium and plutonium from environmental swipe samples for multiple collector inductively coupled plasma mass spectrometry. Anal Chem 90:9441-9448
8. Manard BT, Metzger SC, Rogers KT, Ticknor BW, Bostick DA, Zirakparvar NA, Hexel CR (2020) Exploration of ICP platforms for measuring elemental impurities in uranium ore concentrates. Int J Mass Spectrom:116378
9. Fletcher ND, Manard BT, Metzger SC, Ticknor BW, Bostick DA, Hexel CR (2020) Determining P, S, Br, and I content in uranium by triple quadrupole inductively coupled plasma mass spectrometry. J Radioanal Nucl Chem:1-8
10. Fletcher ND, Manard BT, Bostick DA, Bostick WD, Metzger SC, Ticknor BW, Rogers KT, Hexel CR (2020) Determination of phosphorus and sulfur in uranium ore

concentrates by triple quadrupole inductively coupled plasma mass spectrometry. Talanta:121573. https://doi.org/https://doi.org/10.1016/j.talanta.2020.121573
11. Harouaka K, Hoppe EW, Arnquist IJ (2020) A novel method for measuring ultra-trace levels of U and Th in Au, Pt, Ir, and W matrices using ICP-QQQ-MS employing an O 2 reaction gas. J Anal At Spectrom 35:2859-2866
12. Diez-Fernández S, Isnard H, Nonell A, Bresson C, Chartier F (2020) Radionuclide analysis using collision–reaction cell ICP-MS technology: a review. J Anal At Spectrom 35:2793-2819
13. Jaegler H, Gourgiotis A, Steier P, Golser R, Diez O, Cazala C (2020) Pushing Limits of ICP–MS/MS for the Determination of Ultralow 236U/238U Isotope Ratios. Anal Chem 92:7869-7876
14. Diez-Fernández S, Jaegler H, Bresson C, Chartier F, Evrard O, Hubert A, Nonell A, Pointurier F, Isnard H (2020) A new method for determining 236U/238U isotope ratios in environmental samples by means OF ICP-MS/MS. Talanta 206:120221
15. Manard BT, Bostick DA, Metzger SC, Ticknor BW, Zirakparvar NA, Rogers KT, Hexel CR (2021) Rapid and automated separation of uranium ore concentrates for trace element analysis by inductively coupled plasma – optical emission spectroscopy/triple quadrupole mass spectrometry. Spectrochim Acta B: At Spectrosc 179:106097. https://doi.org/https://doi.org/10.1016/j.sab.2021.106097
16. Matsueda M, Kawakami T, Koarai K, Terashima M, Fujiwara K, Iijima K, Furukawa M, Takagai Y (2022) Using CO2 Reactions to Achieve Mass-spectrometric Discrimination in Simultaneous Plutonium-isotope Speciation with Inductively Coupled Plasma–Tandem Mass Spectrometry. Chem Lett 51:678-682
17. Childs DA, Hill JG (2018) The use of carbon dioxide as the reaction cell gas for the separation of uranium and plutonium in quadrupole inductively coupled plasma mass spectrometry (ICP-MS) for nuclear forensic samples. J Radioanal Nucl Chem 318:139-148
18. Jakubowski N, Moens L, Vanhaecke F (1998) Sector field mass spectrometers in ICP-MS. Spectrochim Acta, Part B 53:1739-1763

19. Boulyga SF, Cunningham JA, Macsik Z, Hiess J, Peńkin MV, Walsh SJ (2017) Development, validation and verification of an ICP-MS procedure for a multi-element analysis of uranium ore concentrates. J Anal At Spectrom 32:2226-2237
20. Marcus RK, Quarles CD, Jr., Barinaga CJ, Carado AJ, Koppenaal DW (2011) Liquid Sampling-Atmospheric Pressure Glow Discharge Ionization Source for Elemental Mass Spectrometry. Anal Chem 83:2425-2429
21. Marcus RK, Manard BT, Quarles CD (2017) Liquid sampling-atmospheric pressure glow discharge (LS-APGD) microplasmas for diverse spectrochemical analysis applications. J Anal At Spectrom 32:704-716
22. Koppenaal DW, Marcus RK (2023) Coupling of the Liquid Sampling–Atmospheric Pressure Glow Discharge to Orbitrap Mass Analyzers for Uranium Isotope Ratio Analysis: Evolution of the Methodology and Implications to the Field. Appl Spectrosc in press
23. Goodwin JV, Manard BT, Ticknor BW, Cable-Dunlap P, Marcus RK (2022) Improved uranium isotopic ratio determinations for the liquid sampling-atmospheric pressure glow discharge orbitrap mass spectrometer by use of moving average processing. J Anal At Spectrom 37:814-822
24. Goodwin JV, Manard BT, Ticknor BW, Cable-Dunlap P, Marcus RK (2023) Initial Characterization and Optimization of the Liquid Sampling-Atmospheric Pressure Glow Discharge Ionization Source Coupled to an Orbitrap Mass Spectrometer for the Determination of Plutonium. Anal Chem
25. Hoegg ED, Godin S, Szpunar J, Lobinski R, Koppenaal DW, Marcus RK (2021) Resolving Severe Elemental Isobaric Interferences with a Combined Atomic and Molecular Ionization Source–Orbitrap Mass Spectrometry Approach: The 87Sr and 87Rb Geochronology Pair. Anal Chem 93:11506-11514
26. Quarles CD, Gonzalez J, Choi I, Ruiz J, Mao X, Marcus RK, Russo RE (2012) Liquid sampling-atmospheric pressure glow discharge optical emission spectroscopy detection of laser ablation produced particles: A feasibility study. Spectrochim Acta B: At Spectrosc 76:190-196. https://doi.org/https://doi.org/10.1016/j.sab.2012.06.048
27. Paing HW, Bryant TJ, Quarles CD, Jr., Marcus RK (2020) Coupling of Laser Ablation and the Liquid Sampling-Atmospheric Pressure Glow Discharge Plasma for

Simultaneous, Comprehensive Mapping: Elemental, Molecular, and Spatial Analysis. Anal Chem 92:12622-12629. https://doi.org/10.1021/acs.analchem.0c02677
28. Marcus RK, Burdette CQ, Manard BT, Zhang LX (2013) Ambient desorption/ionization mass spectrometry using a liquid sampling–atmospheric glow discharge (LS-APGD) ionization source. Anal Bioanal Chem 405:8171-8184. https://doi.org/10.1007/s00216-013-7216-3
29. Marcus RK, Paing HW, Zhang LX (2016) Conceptual Demonstration of Ambient Desorption-Optical Emission Spectroscopy Using a Liquid Sampling-Atmospheric Pressure Glow Discharge Microplasma Source. Anal Chem 88:5579-5584. https://doi.org/10.1021/acs.analchem.6b00751
30. Paing HW, Manard BT, Ticknor BW, Bills JR, Hall KA, Bostick DA, Cable-Dunlap P, Marcus RK (2020) Rapid Determination of Uranium Isotopic Abundance from Cotton Swipes: Direct Extraction via a Planar Surface Reader and Coupling to a Microplasma Ionization Source. Anal Chem 92:8591-8598. https://doi.org/10.1021/acs.analchem.0c01606
31. Bradley VC, Spano TL, Thompson CV, Ticknor BW, Dunlap DR, Metzger SC, Hexel CR, Manard BT (2022) Analysis of solid uranium particulates on cotton swipes with an automated microextraction-ICP-MS system. Anal Methods 14:4466-4473. https://doi.org/10.1039/D2AY01394K
32. Manard BT, Rogers KT, Ticknor BW, Metzger SC, Zirakparvar NA, Roach BD, Bostick DA, Hexel CR (2021) Direct Uranium Isotopic Analysis of Swipe Surfaces by Microextraction-ICP-MS. Anal Chem 93:11133-11139. https://doi.org/10.1021/acs.analchem.1c01569
33. Bradley VC, Spano TL, Metzger SC, Ticknor BW, Dunlap DR, Zirakparvar NA, Roach BD, Hexel CR, Manard BT (2022) Direct isotopic analysis of solid uranium particulates on cotton swipes by microextraction-ICP-MS. Anal Chim Acta 1209:339836. https://doi.org/https://doi.org/10.1016/j.aca.2022.339836
34. Manard BT, Metzger SC, Rogers KT, Ticknor BW, Zirakparvar NA, Roach BD, Bostick DA, Hexel CR (2021) Direct analysis of cotton swipes for plutonium isotope determination by microextraction-ICP-MS. J Anal At Spectrom 36:2202-2209. https://doi.org/10.1039/D1JA00255D

35. Hoegg ED, Marcus RK, Hager GJ, Hart GL, Koppenaal DW (2018) Concomitant ion effects on isotope ratio measurements with liquid sampling – atmospheric pressure glow discharge ion source Orbitrap mass spectrometry. J Anal At Spectrom 33:251-259. https://doi.org/10.1039/C7JA00308K
36. Richter S, Venchiarutti C, Hennessy C, Jacobsson U, Bujak R, Truyens J, Aregbe Y (2018) Preparation and certification of the uranium nitrate solution reference materials series IRMM-2019 to IRMM-2029 for the isotopic composition. J Radioanal Nucl Chem 318:1359-1368. https://doi.org/10.1007/s10967-018-6166-9
37. Mathew K, O'Connor G, Hasozbek A, Kraiem M (2013) Total evaporation method for uranium isotope-amount ratio measurements. J Anal At Spectrom 28:866-876
38. Hoegg ED, Williams TJ, Bills JR, Marcus RK, Koppenaal DW (2020) A multi-electrode glow discharge ionization source for atomic and molecular mass spectrometry. J Anal At Spectrom 35:1969-1978. https://doi.org/10.1039/D0JA00142B
39. Hoegg ED, Manard BT, Wylie EM, Mathew KJ, Ottenfeld CF, Marcus RK (2019) Initial Benchmarking of the Liquid Sampling-Atmospheric Pressure Glow Discharge-Orbitrap System Against Traditional Atomic Mass Spectrometry Techniques for Nuclear Applications. J Am Soc Mass Spectrom 30:278-288. https://doi.org/10.1007/s13361-018-2071-2
40. Thomas R (2013) Practical Guide to ICP-MS: A Tutorial Guide for Beginners. CRC Press, Boca Raton
41. Olesik JW, Jones DR (2006) Strategies to develop methods using ion-molecule reactions in a quadrupole reaction cell to overcome spectral overlaps in inductively coupled plasma mass spectrometry. J Anal At Spectrom 21:141-159
42. Yamada N, Takahashi J (2018) Evolution of Collision/Reaction Cell Technology - Advent of Triple Quadrupole ICP-MS. Bunseki Kagaku 67:249-279. https://doi.org/10.2116/bunsekikagaku.67.249
43. Williams TJ, Hoegg ED, Bills JR, Marcus RK (2021) Roles of collisional dissociation modalities on spectral composition and isotope ratio measurement performance of the liquid sampling – atmospheric pressure glow discharge / orbitrap mass spectrometer coupling. Int J Mass Spectrom 464:116572. https://doi.org/https://doi.org/10.1016/j.ijms.2021.116572

44. Cox KA, Cleven CD, Cooks RG (1995) Mass shifts and local space charge effects observed in the quadrupole ion trap at higher resolution. Int J Mass Spectrom 144:47-65. https://doi.org/https://doi.org/10.1016/0168-1176(95)04152-B
45. Gorshkov MV, Fornelli L, Tsybin YO (2012) Observation of ion coalescence in Orbitrap Fourier transform mass spectrometry. Rapid Commun Mass Spectrom 26:1711-1717. https://doi.org/https://doi.org/10.1002/rcm.6289
46. Bills JR, Nagornov KO, Kozhinov AN, Williams TJ, Tsybin YO, Marcus RK (2021) Improved Uranium Isotope Ratio Analysis in Liquid Sampling–Atmospheric Pressure Glow Discharge/Orbitrap FTMS Coupling through the Use of an External Data Acquisition System. J Am Soc Mass Spectrom 32:1224-1236. https://doi.org/10.1021/jasms.1c00051

Figure Captions:

Figure 1: Schematic representation of the key components of the dual-electrode LS-APGD source and Orbitrap mass spectrometer platform.

Figure 2: Mass spectra of Pb (10 mg mL^{-1}) a) without and b) with 90 eV of CID. The shaded region in both figures represents the typical settings for the quadrupole range used for uranium isotope ratio determinations with this platform.

Figure 3: Mass spectra of Pt (10 mg mL^{-1}) a) without and b) with 90 eV of CID. The shaded region in both figures represents the typical settings for the quadrupole range used for uranium isotope ratio determinations with this platform.

Figure 4: Mass spectra of Ta (10 mg mL^{-1}) a) without and b) with 90 eV of CID. The shaded region in both figures represents the typical settings for the quadrupole range used for uranium isotope ratio determinations with this platform.

Figure 5: Mass spectra of W (10 mg mL^{-1}) a) without and b) with 90 eV of CID. The shaded region in both figures represents the typical settings for the quadrupole range used for uranium isotope ratio determinations with this platform.

Figure 6: Comparison of the mass spectra of Pb (10 mg mL^{-1}) with and without 120 eV HCD after applying 90 eV of CID. The red line represents the mass spectrum of lead without HCD (90 eV CID only), and the black line represents the mass spectrum of lead with 90 eV CID and 120 eV of HCD. The insert is an expanded region illustrating the reduction in lead species between 215-300 m/z with HCD and CID over the CID only case.

Figure 7: Mass spectra of low-enriched uranium (10 ng mL^{-1}) with 1000X concentrations (10 mg mL^{-1}) of a) Pt, b) Pb, c) Ta, and d) W. The inserts illustrate expanded regions around the signal for ^{235}U and ^{238}U.

Figure 8: Uranium Isotope ratios obtained from neat and from spiked uranium IRMM-2028 isotopic standards. The average isotope ratio for the un-spiked case is represented by the solid blue line, and the standard deviation for n=5 determinations is represented by the dashed blue lines. The intra-measurement standard deviation is shown.

Graphical Abstract

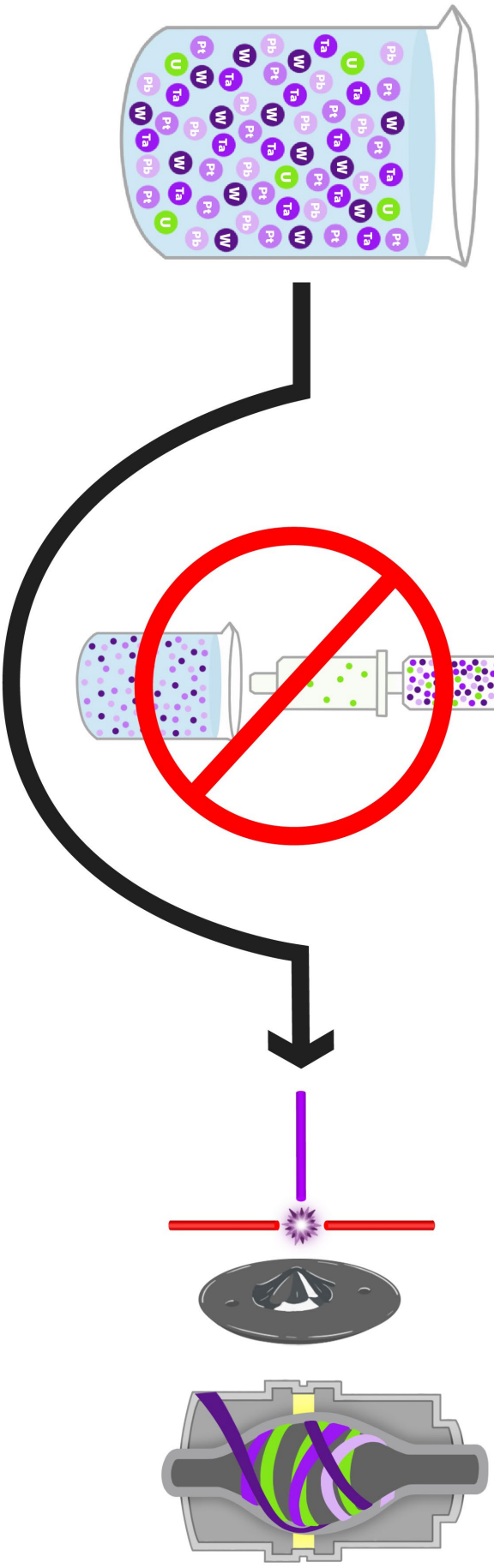

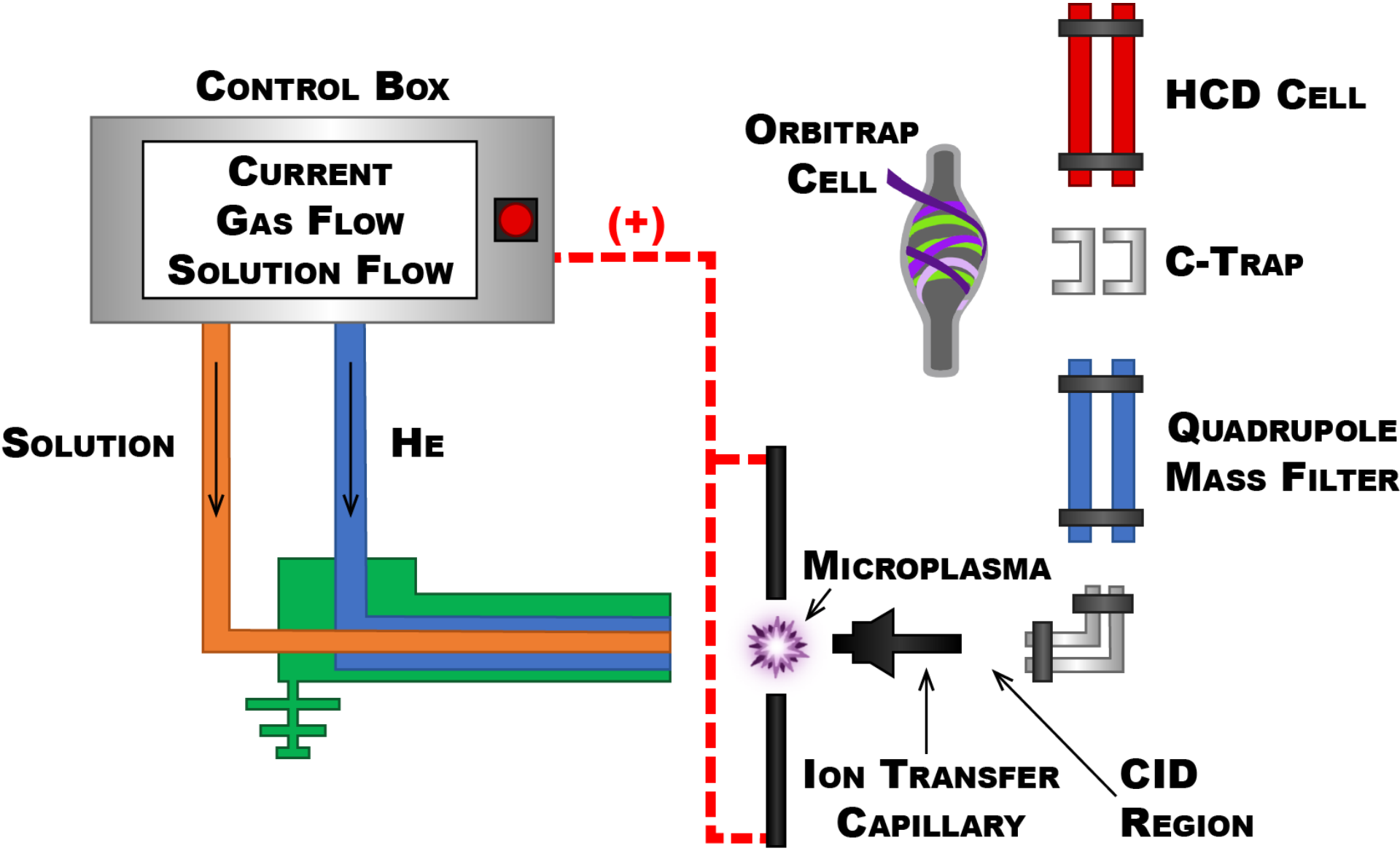
Control Box
Current
Gas Flow
Solution Flow
(+)
Solution
He
Orbitrap
Cell
HCD Cell
C-Trap
Quadrupole
Mass Filter
Microplasma
Ion Transfer
Capillary
CID
Region

Fig 1

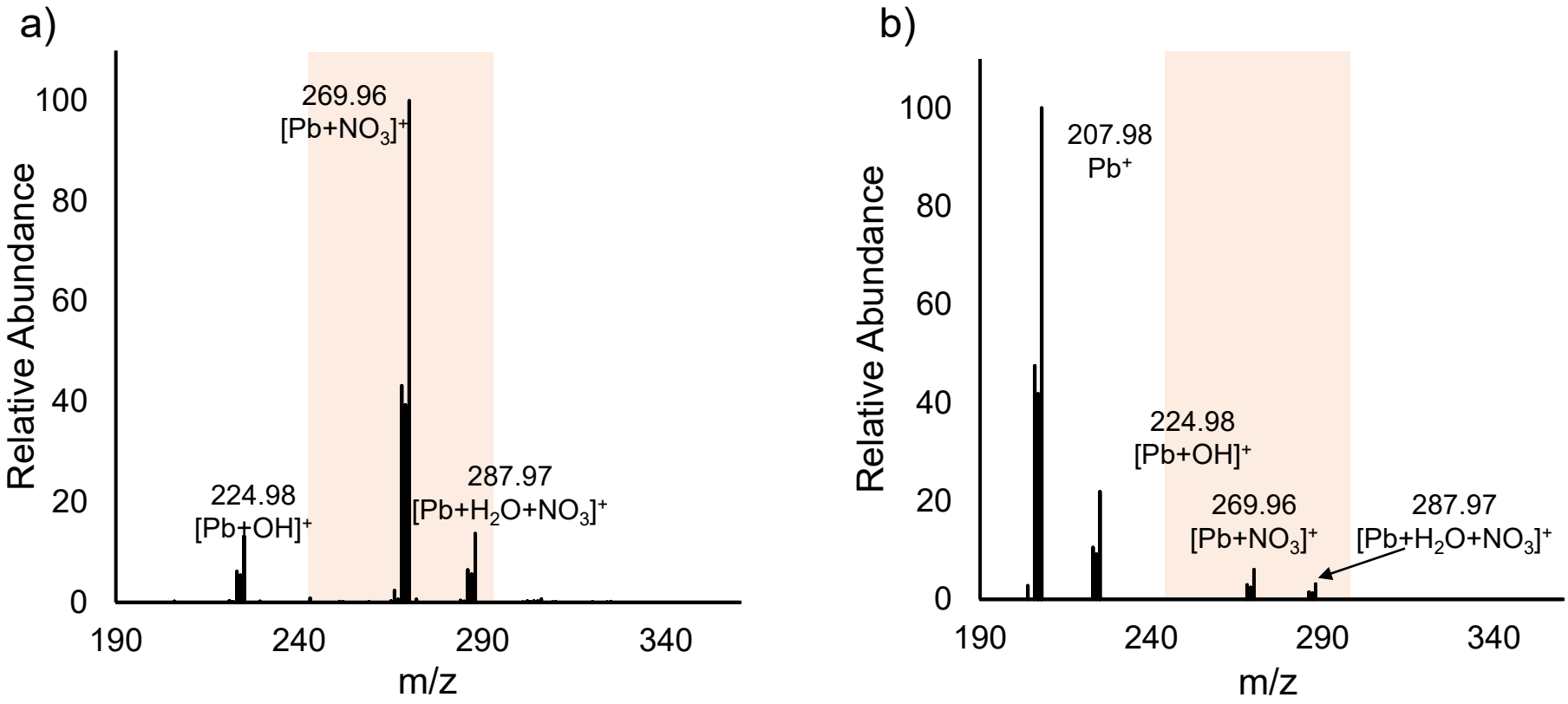
a)
Relative Abundance
100
80
60
40
20
0
190
240
290
340
m/z
269.96
[Pb+NO3]+
224.98
[Pb+OH]+
287.97
[Pb+H2O+NO3]+
b)
Relative Abundance
100
80
60
40
20
0
190
240
290
340
m/z
207.98
Pb+
224.98
[Pb+OH]+
269.96
[Pb+NO3]+
287.97
[Pb+H2O+NO3]+

Fig 2

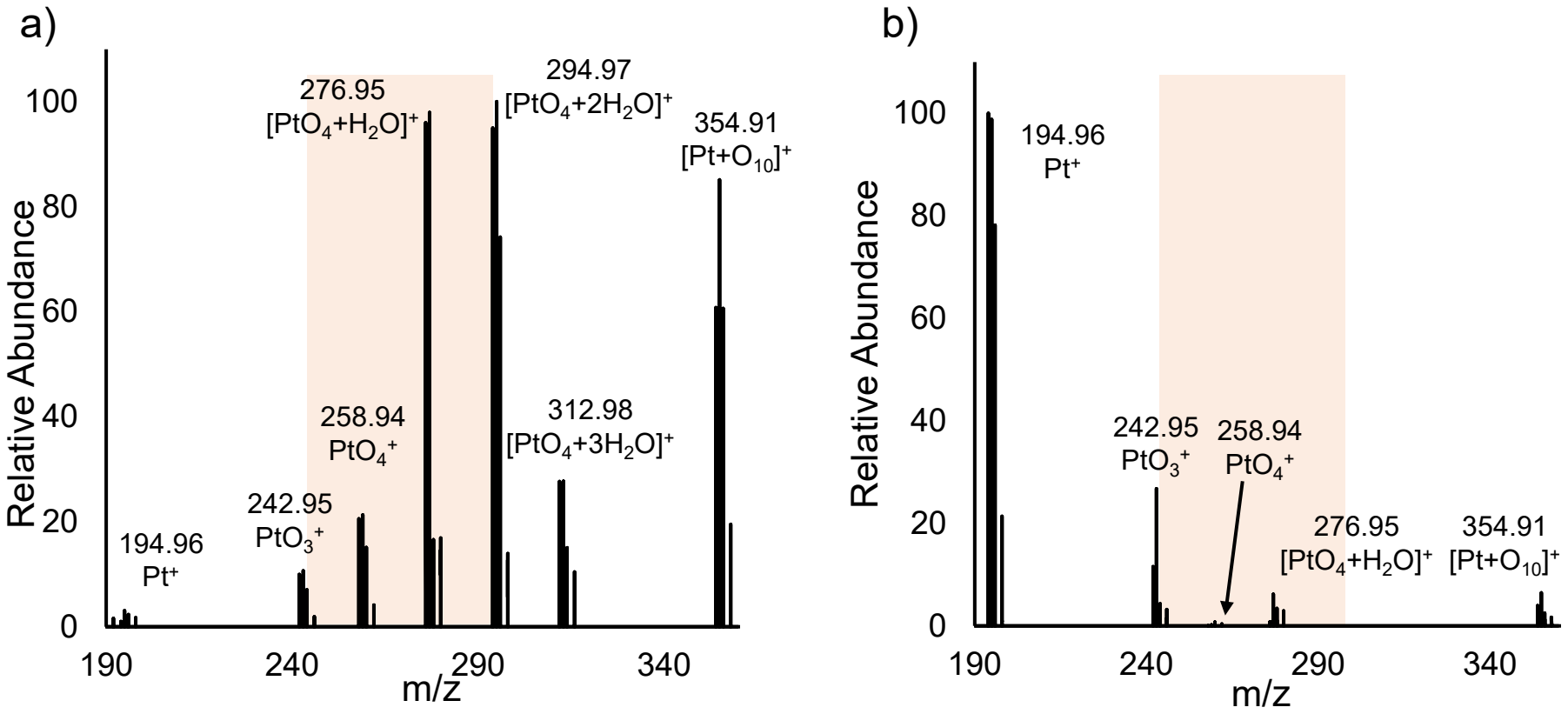
a)
Relative Abundance
100
80
60
40
20
0
190
240
290
340
m/z
194.96
Pt+
242.95
PtO3+
258.94
PtO4+
276.95
[PtO4+H2O]+
294.97
[PtO4+2H2O]+
312.98
[PtO4+3H2O]+
354.91
[Pt+O10]+
b)
Relative Abundance
100
80
60
40
20
0
190
240
290
340
m/z
194.96
Pt+
242.95
PtO3+
258.94
PtO4+
276.95
[PtO4+H2O]+
354.91
[Pt+O10]+

Fig 3

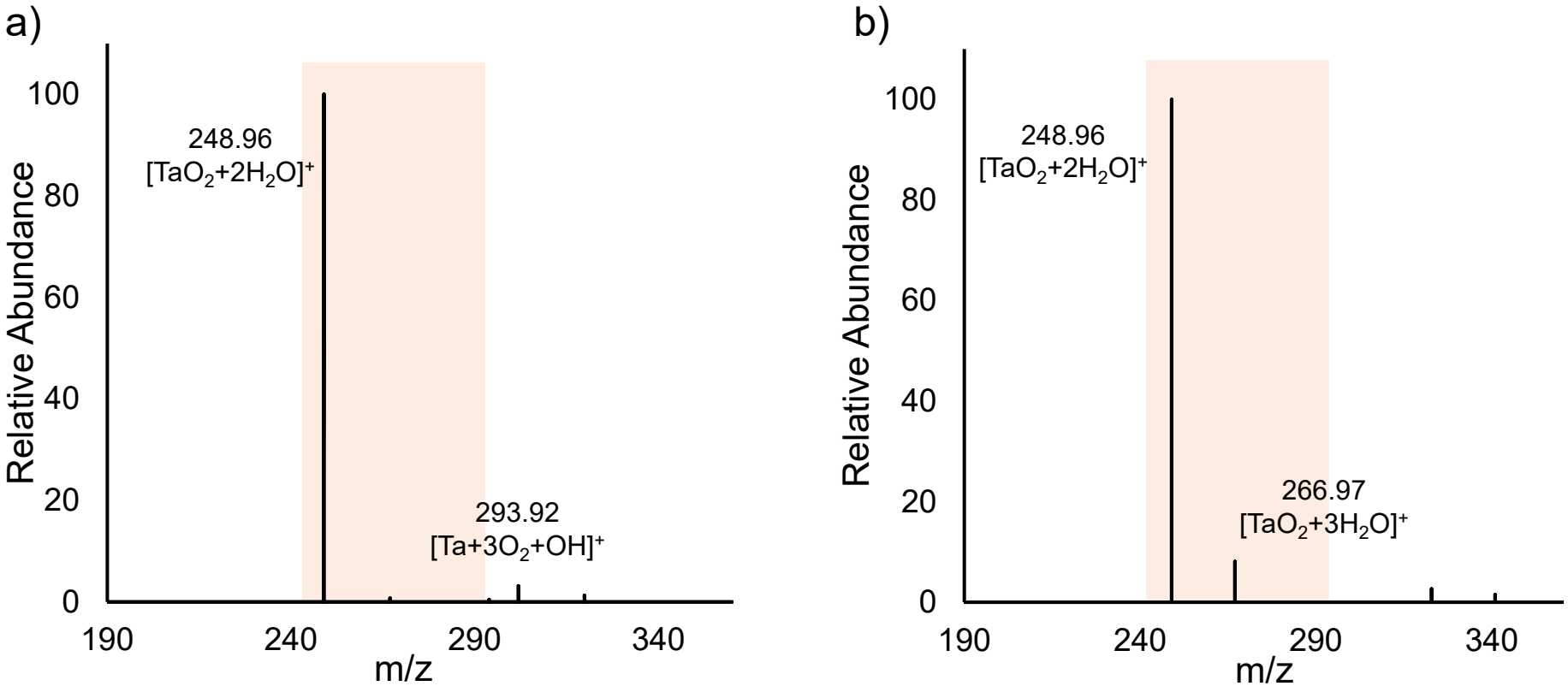
a)
Relative Abundance
100
80
60
40
20
0
248.96
[TaO2+2H2O]+
293.92
[Ta+3O2+OH]+
190
240
290
340
m/z
b)
Relative Abundance
100
80
60
40
20
0
248.96
[TaO2+2H2O]+
266.97
[TaO2+3H2O]+
190
240
290
340
m/z

Fig 4

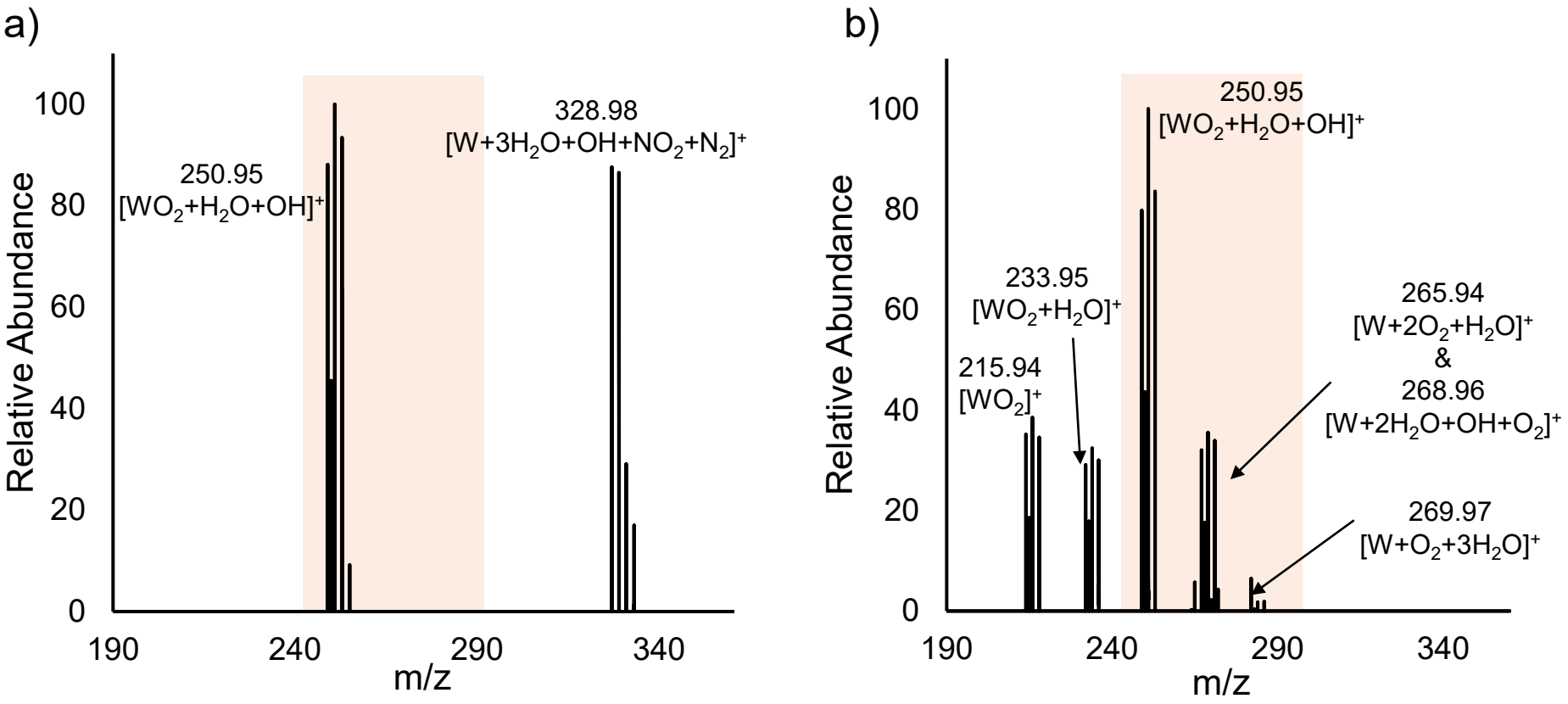
a)
Relative Abundance
100
80
60
40
20
0
190
240
290
340
m/z
250.95
[WO2+H2O+OH]+
328.98
[W+3H2O+OH+NO2+N2]+
b)
Relative Abundance
100
80
60
40
20
0
190
240
290
340
m/z
250.95
[WO2+H2O+OH]+
233.95
[WO2+H2O]+
215.94
[WO2]+
265.94
[W+2O2+H2O]+
&
268.96
[W+2H2O+OH+O2]+
269.97
[W+O2+3H2O]+

Fig 5

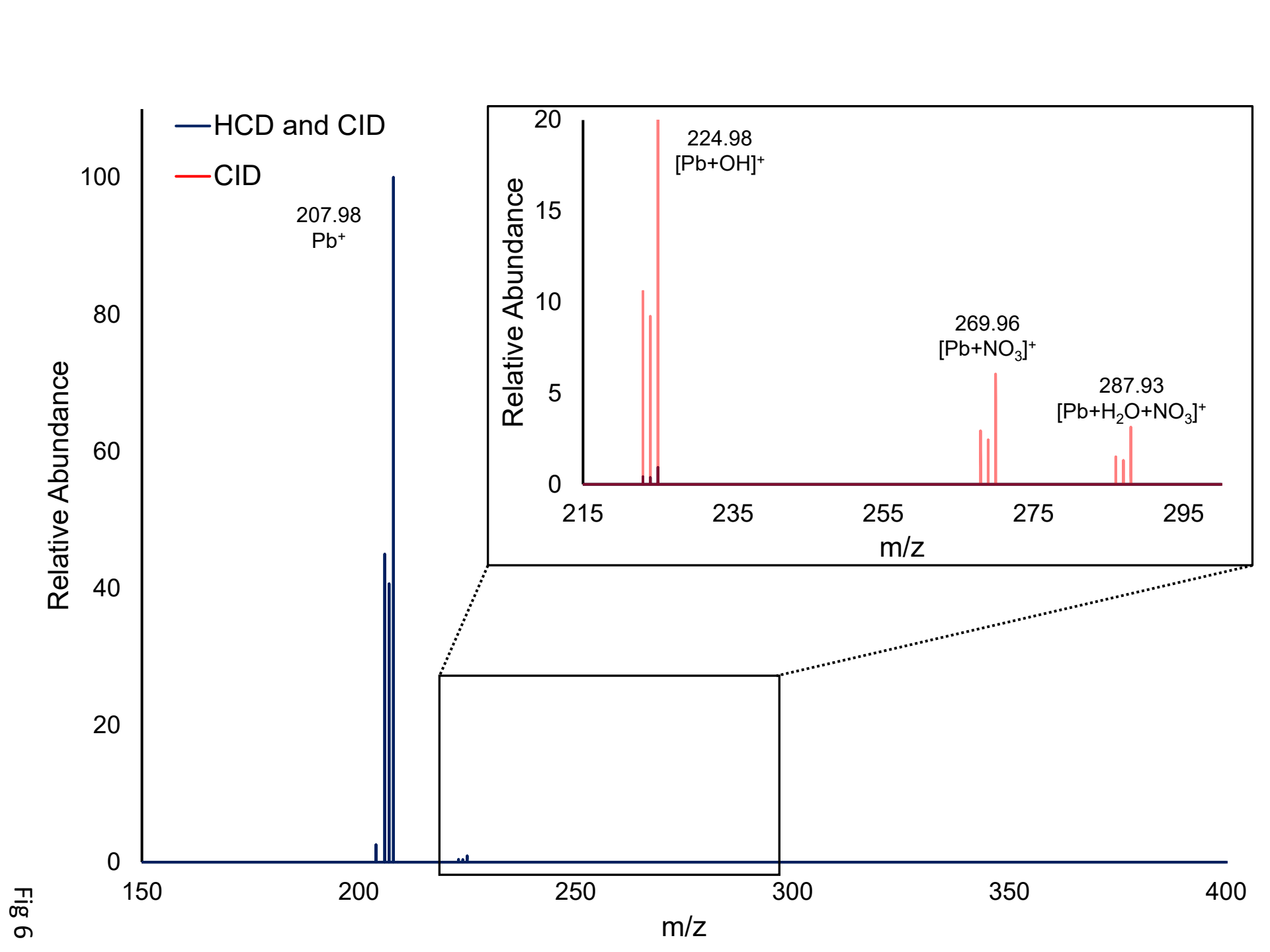
HCD and CID
CID
207.98
Pb+
Relative Abundance
m/z
224.98
[Pb+OH]+
269.96
[Pb+NO3]+
287.93
[Pb+H2O+NO3]+

Fig 6

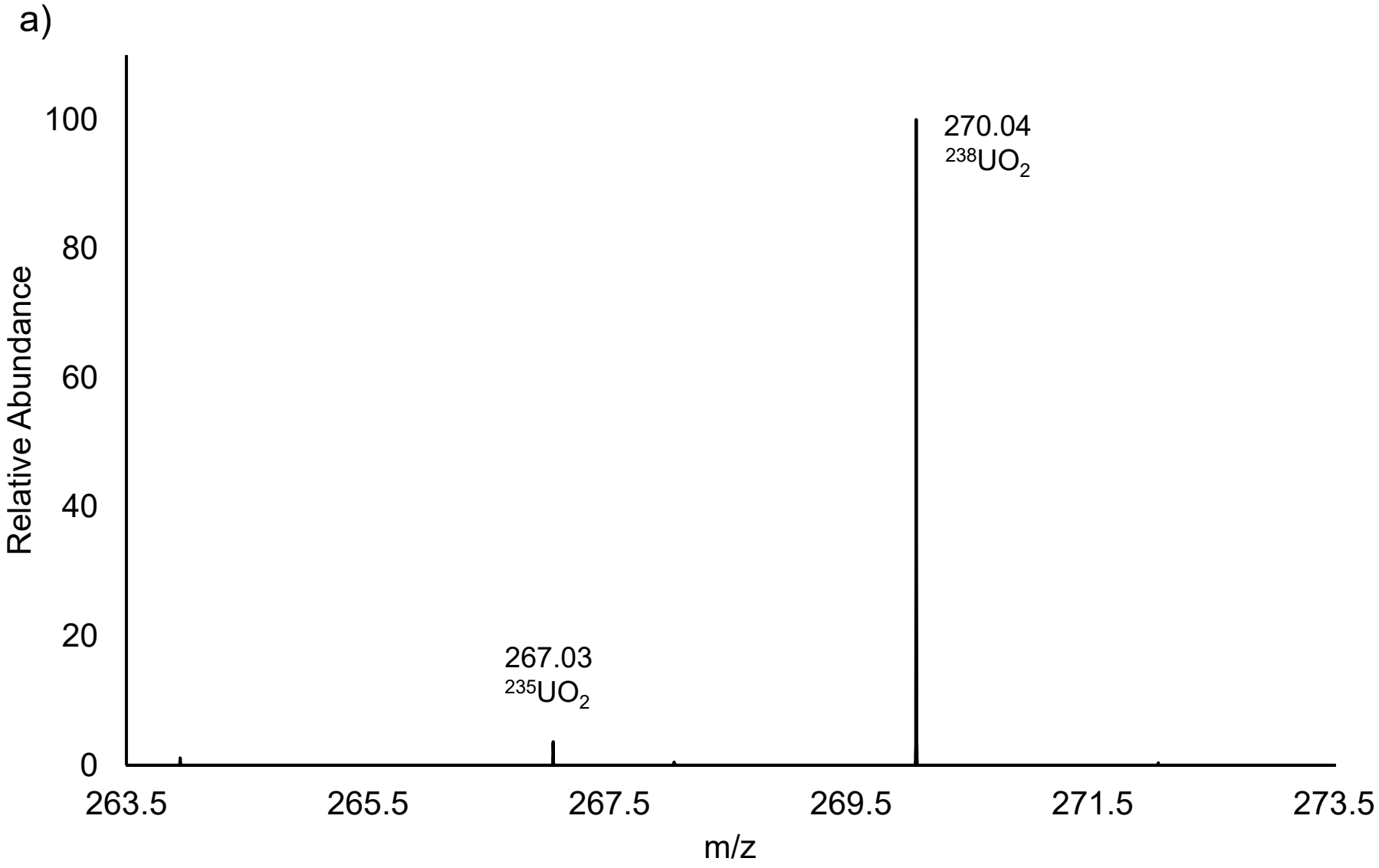
a)
100
80
60
40
20
0
Relative Abundance
270.04
$^{238}UO_2$
267.03
$^{235}UO_2$
263.5
265.5
267.5
269.5
271.5
273.5
m/z

Fig 7a

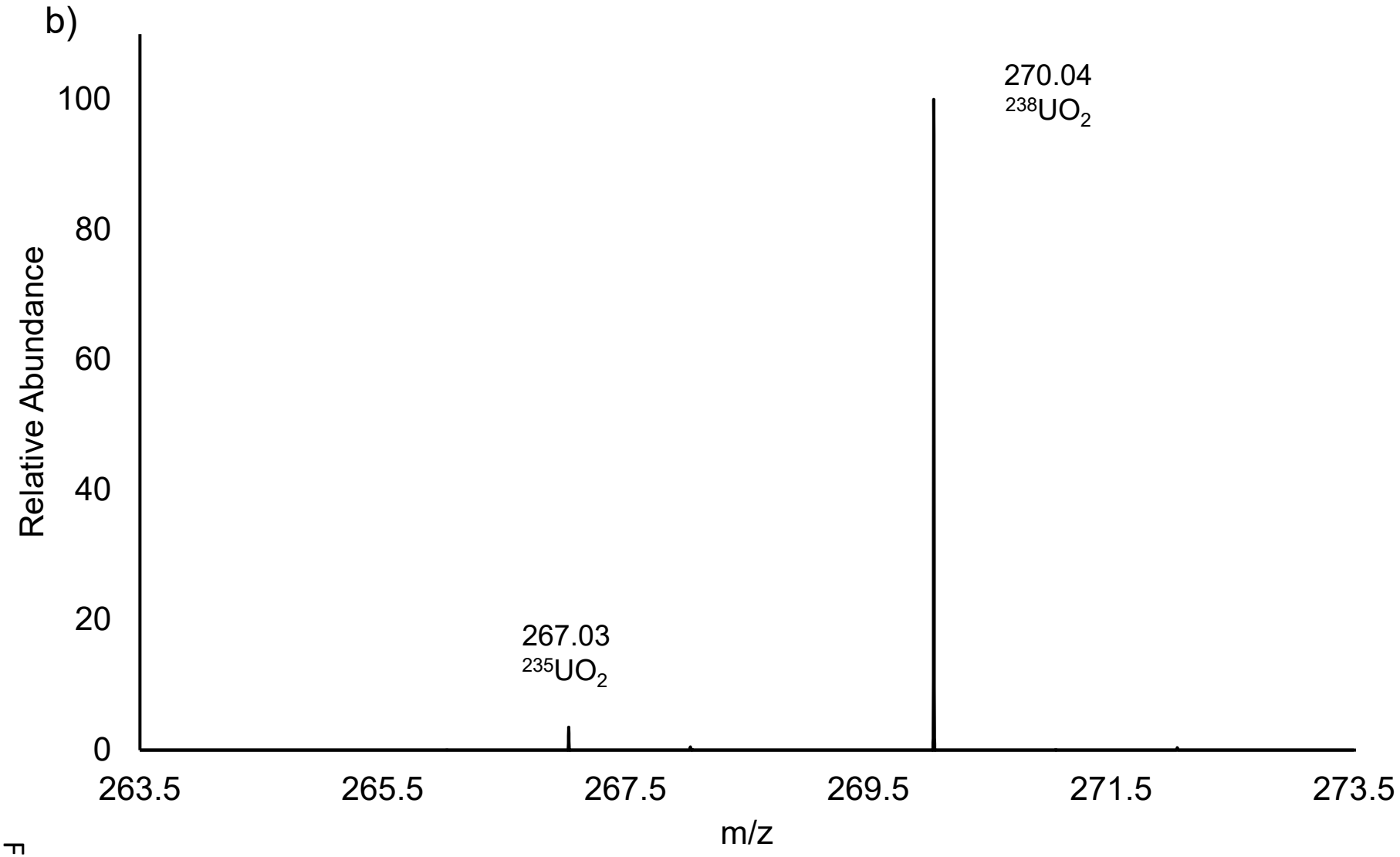
b)
100
80
60
40
20
0
Relative Abundance
270.04
238UO2
267.03
235UO2
263.5
265.5
267.5
269.5
271.5
273.5
m/z

Fig 7b

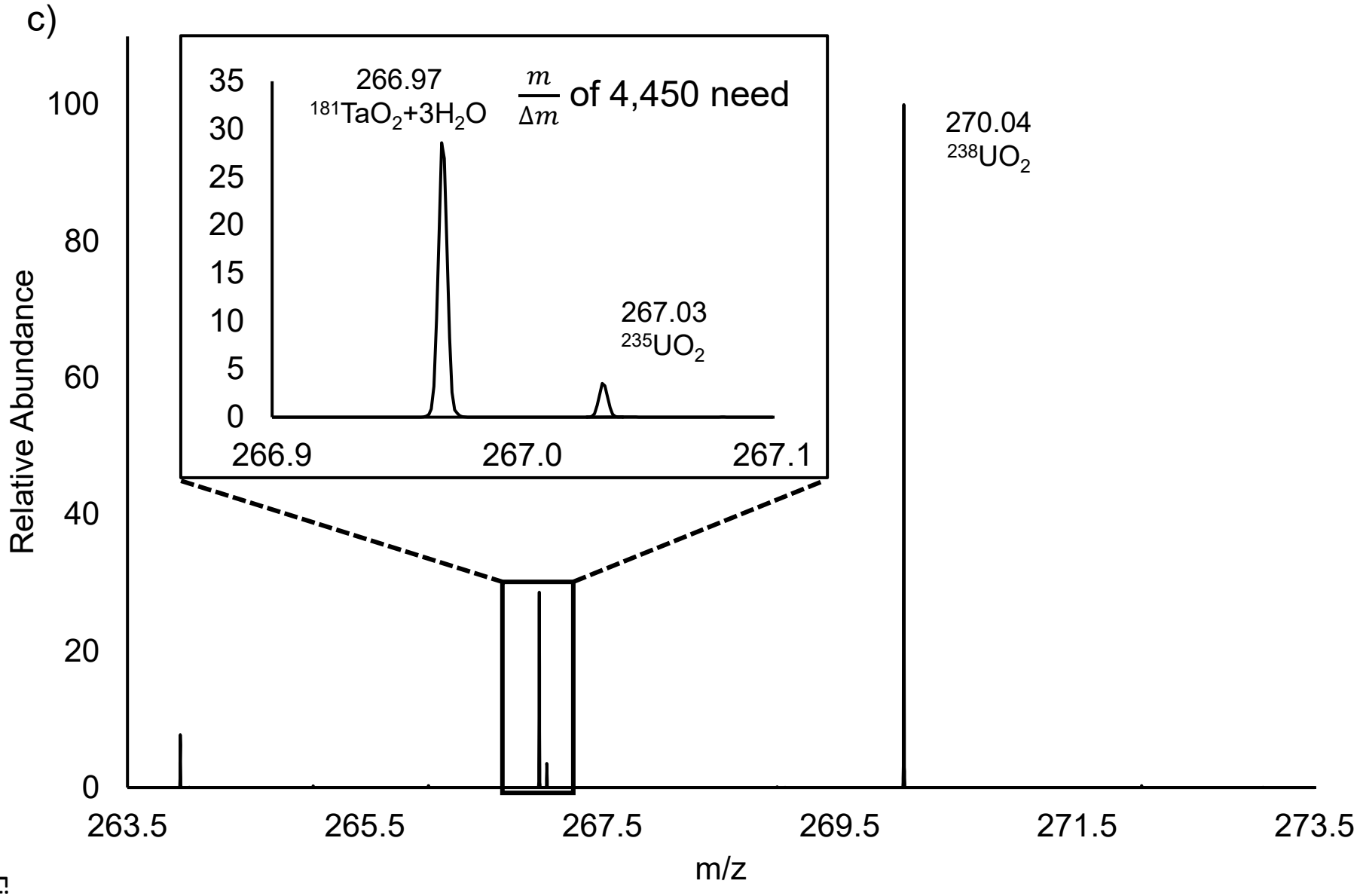
c)
Relative Abundance
m/z
100
80
60
40
20
0
263.5
265.5
267.5
269.5
271.5
273.5
270.04
$^{238}UO_2$
266.97
$^{181}TaO_2$+3H_2O
$\frac{m}{\Delta m}$ of 4,450 need
267.03
$^{235}UO_2$
35
30
25
20
15
10
5
0
266.9
267.0
267.1

Fig 7c

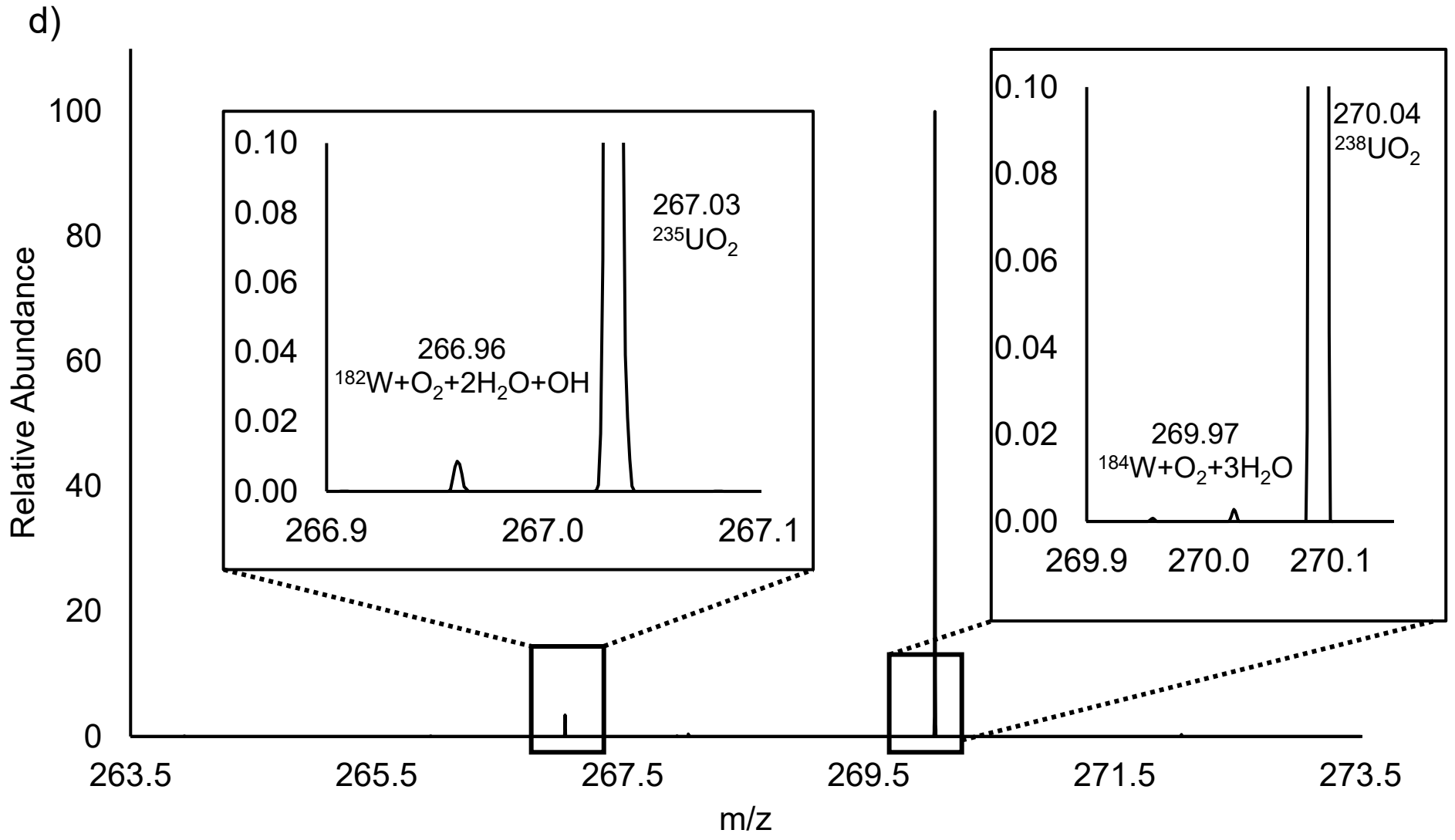
d)
Relative Abundance
100
80
60
40
20
0
263.5
265.5
267.5
269.5
271.5
273.5
m/z
0.10
0.08
0.06
0.04
0.02
0.00
266.9
267.0
267.1
267.03
$^{235}UO_2$
266.96
$^{182}W+O_2+2H_2O+OH$
0.10
0.08
0.06
0.04
0.02
0.00
269.9
270.0
270.1
270.04
$^{238}UO_2$
269.97
$^{184}W+O_2+3H_2O$

Fig 7d

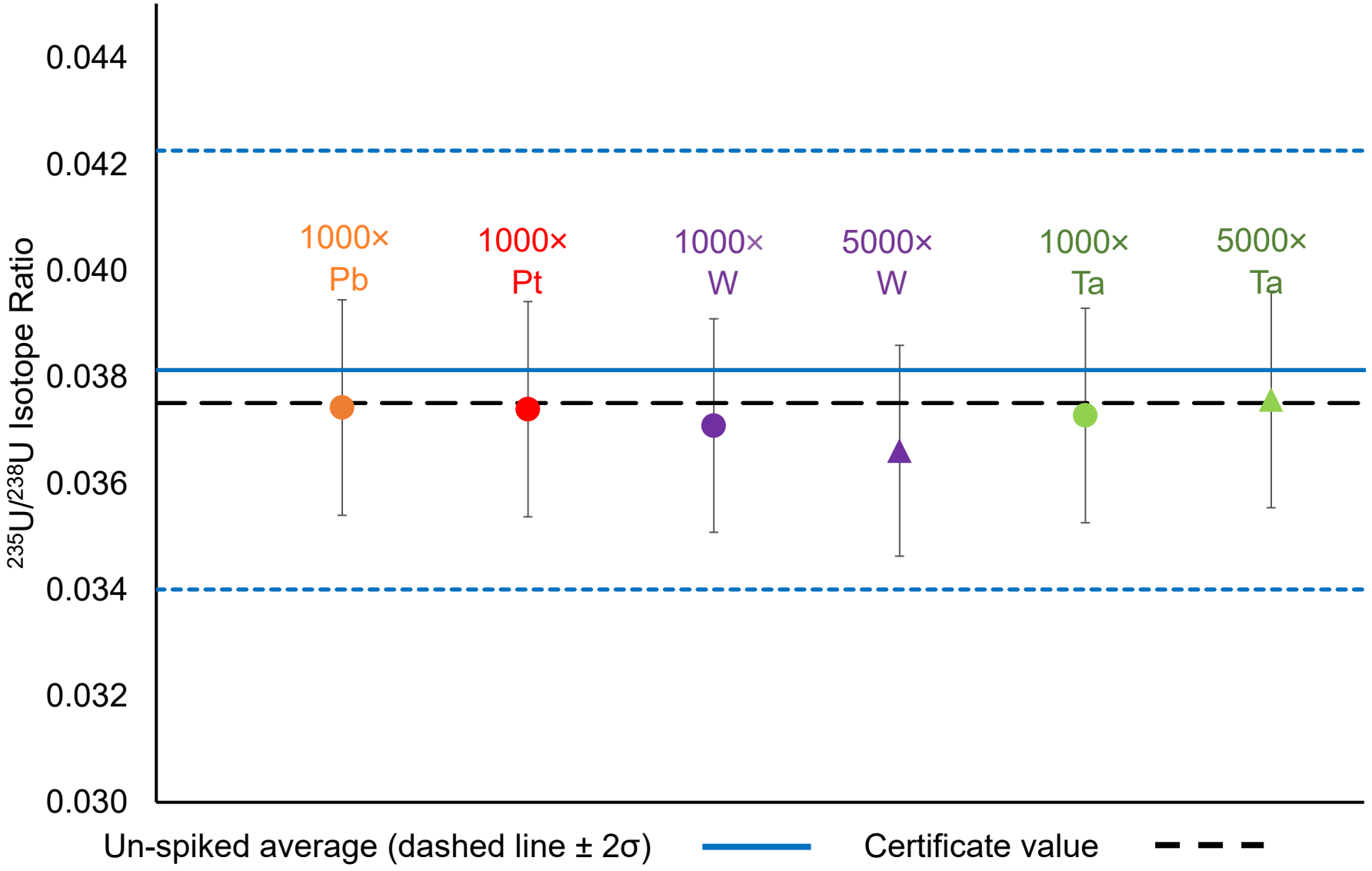
0.044
0.042
0.040
0.038
0.036
0.034
0.032
0.030
$^{235}U/^{238}U$ Isotope Ratio
1000× Pb
1000× Pt
1000× W
5000× W
1000× Ta
5000× Ta
Un-spiked average (dashed line ± 2σ)
Certificate value

Fig 8